Quantitative Biology
DOI 10.1007/s40484-016-0086-x

RESEARCH ARTICLE

A resistant method for landmark-based analysis of individual asymmetry in two dimensions

Sebastián Torcida[1,*], Paula Gonzalez[2] and Federico Lotto[3]

[1] Dpto. Matemática-Exactas, UNCPBA. Tandil 7000, Argentina.
[2] Fac. de Ciencias Naturales y Museo, UNLP-CONICET. La Plata 1900, Argentina
[3] Instituto de Veterinaria Ing. Fernando N. Dulout (IGEVET), Facultad de Cs. Veterinarias, UNLP-CONICET. La Plata 1900, Argentina
* Correspondence: unisebas@gmail.com

Received April 3, 2016; Revised June 17, 2016; Accepted August 27, 2016

***Background*: Symmetry of biological structures can be thought as the repetition of their parts in different positions and orientations. Asymmetry analyses, therefore, focuses on identifying and measuring the location and extent of symmetry departures in such structures. In the context of geometric morphometrics, a key step when studying morphological variation is the estimation of the symmetric shape. The standard procedure uses the least-squares Procrustes superimposition, which by averaging shape differences often underestimates the symmetry departures thus leading to an inaccurate description of the asymmetry pattern. Moreover, the corresponding asymmetry values are neither geometrically intuitive nor visually perceivable.**

***Methods*: In this work, a resistant method for landmark-based asymmetry analysis of individual bilateral symmetric structures in 2D is introduced. A geometrical derivation of this new approach is offered, while its advantages in comparison with the standard method are examined and discussed through a few illustrative examples.**

***Results*: Experimental tests on both artificial and real data show that asymmetry is more effectively measured by using the resistant method because the underlying symmetric shape is better estimated. Therefore, the most asymmetric (respectively symmetric) landmarks are better determined through their large (respectively small) residuals. The percentage of asymmetry that is accounted for by each landmark is an additional revealing measure the new method offers which agrees with the displayed results while helping in their biological interpretation.**

***Conclusions*: The resistant method is a useful exploratory tool for analyzing shape asymmetry in 2D, and it might be the preferable method whenever a non homogeneous deformation of bilateral symmetric structures is possible. By offering a more detailed and rather exhaustive explanation of the asymmetry pattern, this new approach will hopefully contribute to improve the quality of biological or developmental inferences.**

Keywords: resistant procrustes method; shape asymmetry; matching and object symmetry; landmarks

INTRODUCTION

Many biological structures exhibit some kind of *symmetry*: i.e., the repetition of their parts in different positions and orientations. Typically, these repeated parts are not exact copies from each other but differ in their morphological or histological characteristics (e.g., size, shape, number and composition of cells). *Shape asymmetry*, as the study of departures from symmetry of symmetric structures, is of great interest in different areas such as biology and medicine; the analysis of the magnitude and/or the direction of asymmetry is routinely applied when assessing pathological conditions and the effect of genetic and environmental factors on the development of phenotypic traits [1–3].

The quantitative evaluation of asymmetry has been mostly based on linear measurements of continuous traits and the counting of discrete traits [4]. More recently, the

application of geometric morphometric techniques in shape asymmetry analyses has shown some advantages over other approaches [5–15]. Geometric morphometrics assumes that Cartesian coordinates of landmarks capture the essential information about the morphology of individuals, describing also the position and orientation of specimens; landmark-based methods are then used to analyze and explain shape variation.

A central issue in landmark-based methods is which criterion should be used to align the configurations of landmarks under analysis, because the exhibited shape differences highly depend on the chosen superimposition [10,16–19]. The least-squares (LS) Procrustes method allows atypically large deformations to have a big impact on the alignment, and thus may obscure true shape differences. Moreover, by spreading shape differences among landmarks the LS method simultaneously underestimates variation in some parts of the structure and overestimates it in others. It is acknowledged that whenever shape variation is not homogeneously distributed (the underlying assumption of the LS method) but instead concentrated in some anatomical traits a *resistant* Procrustes superimposition is better in helping to identify those regions where shape differences are in fact located [17–21]. Among other distinctive features resistant methods are specifically designed to capture the main trend or pattern from data [23–25], thus limiting the influence of atypical values or errors; following a resistant superimposition [20,21], the matching tends to be close in similar regions and not close in the relatively deformed ones. In this way, resistant techniques are more effective than LS methods in assessing shape differences.

The analysis of shape asymmetry in a geometric morphometrics framework typically uses the LS Procrustes superimposition as the standard alignment criterion [7,8,11–13,26]. This method minimizes the sum of squared Euclidean distances between the Cartesian coordinates of corresponding landmarks after superimposition, and the magnitude of the resulting shape asymmetry is estimated by the squared root of this sum which is known as Procrustes distance. A major drawback of the LS Procrustes superimposition is to average shape variation among landmarks [17,20,22] although many morphometric studies expect variability to be placed at specific points from structures [21,27–29]. Moreover, following a LS superimposition the Procrustes distance is neither geometrically intuitive nor visually perceivable when the results are graphically displayed: its value does not properly quantify the exhibited lack of fit. Procrustes distance is actually meaningful in the abstract non-Euclidean (curved) shape space of LS superimposed configurations which in turn differs from Kendall's non-Euclidean shape space (both shape spaces can be exactly matched only under very restricted assumptions: configurations of only three landmarks; [30]). A projection of the LS results onto a tangent Euclidean (flat) space is typically used as an additional approximation that enables standard linear (flat) multivariate analyses on the LS residuals.

Based on these considerations, a resistant method for the study of shape asymmetry via anatomical landmarks is introduced. More specifically, a resistant estimate of the *symmetric shape* (also known as the *component of symmetric variation*) from a single configuration of landmarks in two dimensions is obtained and used afterwards to analyze and measure shape asymmetry within individuals. Due to its widespread interest, structures with *bilateral symmetry* are in particular considered: these are made of two mirror copies at opposite sides of the body. Two forms of bilateral symmetry are commonly distinguished: *matching symmetry*, where the two mirror images are considered separated parts of the structure (e.g., fly wings), and *object symmetry*, where the two mirror images are located at each side of an axis (plane) named the *median* or *sagittal axis* (median plane in three dimensions) which also composes the whole structure (e.g., human face).

RESULTS

The analysis of shape variation of a single structure with matching symmetry focuses on the repeated parts and does not consider the combined structure as a whole: the structure is thought to be divided into two separated parts that are approximate mirror images from each other. In two dimensions, the Cartesian coordinates of m selected landmarks are recorded on each of these parts; as a result two m by 2 matrices $\boldsymbol{L}$ (left, say) and $\boldsymbol{R}$ (right), one for each side of the structure, are used to store in their rows the Cartesian coordinates of corresponding landmarks. The median axis is usually not included neither in data nor in the analysis [13].

The analysis of shape variation of a single structure with two-dimensional object symmetry is instead based on a single configuration of landmarks that includes information from both mirror parts and also from the median axis passing through the structure. Two types of landmarks are in this case distinguished: *paired* and *unpaired* landmarks. Paired landmarks occur on each of the repeated parts and outside the median axis (e.g., in a human face, the corresponding corners of the mouth or the eye). Unpaired landmarks, in turn, are placed at the median axis (e.g., in a human face, the tip from the nose and the chin). A single m by 2 matrix $\boldsymbol{X}$ whose rows are the Cartesian coordinates of the m selected landmarks stores this information from the whole structure. Without loss of generality, it can be assumed the storing pattern in $\boldsymbol{X}$ is the following: the first s rows correspond to the

Cartesian coordinates from the unpaired landmarks; the next q rows (from $s+1$ to $s+q$) correspond to the Cartesian coordinates from the e.g. left paired landmarks, while the last q rows (from $s+q+1$ to $s+2q$) in $\boldsymbol{X}$ correspond to the Cartesian coordinates from the remaining right paired landmarks. Thus, $m = s + 2q$ where s and q denote the number of unpaired and paired landmarks, respectively.

Symmetric shape estimation within individuals: the standard LS Procrustes method

Matching symmetry

To extract information on shape asymmetry from single structures with matching symmetry, a reasonable strategy is to try to optimally match the two separated mirror copies (e.g., left and right wings) represented by matrices $\boldsymbol{L}$ and $\boldsymbol{R}$; the resulting differences can be afterwards attributed to asymmetry. If differences in size between the two mirror parts are detected in the process, they are thought to be caused by (centroid) size asymmetry. This type of asymmetry is different from shape asymmetry, and both are usually assumed independent and analyzed accordingly [12].

The LS Procrustes superimposition [31,32] is the commonly chosen strategy to achieve the optimal matching between mirror parts $\boldsymbol{L}$ and $\boldsymbol{R}$ [11,13]. Intuitively, a reflection should serve to optimally match two mirror images; this suggests that a more restricted version of the LS Procrustes superimposition, specifically considering translation, scale and reflection transformations, could be used instead when shape variation under matching symmetry is analyzed (recall that a rotation transformation can be obtained as a combination of two reflections, but not conversely).

In studies of asymmetry, the Procrustes method usually proceeds in several steps [7,13,15,26,33]. The standard LS Procrustes procedure for quantifying departures from matching symmetry within individuals via landmarks is [11]:

(i) For a preliminary orientation matching, reflect the landmark configuration from on one side onto its mirror image (e.g., reflect the left wing onto the right one) by reversing the sign of one of the Cartesian coordinates (e.g., change the sign of the x coordinate from matrix $\boldsymbol{L}$; this step turns out to be unnecessary since the optimal orientation agreement can be achieved in the next step through a reflection transformation, if needed).

(ii) Perform a LS Procrustes superimposition of configurations $\boldsymbol{L}$ and $\boldsymbol{R}$.

(iii) Estimate the symmetric shape as the average between the two optimally fitted configurations.

(iv) Measure the resulting shape asymmetry as the Procrustes distance between the optimally fitted configurations, or equivalently (up to a factor of 2), through the Procrustes distance between one of them and the estimated symmetric shape.

Object symmetry

Under object symmetry, the two mirror halves belong to a whole structure and are thus interdependent. Because only one landmark configuration is available, a mirror copy of it needs to be created if a superimposition is to be performed. Unlike matching asymmetry, any difference between the two mirror sides (including differences in size) is considered a property of the whole structure and thus a specific analysis of size asymmetry does not make sense in this case.

A procedure to study variation and asymmetry of shapes with internal symmetry was briefly outlined by Bookstein [10] and Auffray *et al.* [8]. The standard LS Procrustes procedure to quantify departures from object symmetry within individuals via landmarks consists of these steps [11]:

(i) Generate a mirror copy $\mathbf{Z}$ of configuration $\mathbf{X}$ by reversing the sign of one of the Cartesian coordinates in $\mathbf{X}$ (e.g., change the sign of the x coordinate). Each paired landmark from the reflected copy is then relabeled to obtain the label of its counterpart; corresponding rows from matrices $\mathbf{X}$ and $\mathbf{Z}$ will in this way describe landmarks lying on the same side from the median axis.

(ii) Perform a LS Procrustes superimposition between $\mathbf{X}$ and its reflected copy $\mathbf{Z}$

(iii) Estimate the symmetric shape as the average between the two optimally fitted configurations, which is perfectly symmetrical

(iv) The resulting shape asymmetry of the whole structure is finally measured through the Procrustes distance between the fitted configurations, or equivalently (up to a factor of 2), through the Procrustes distance between the original configuration $\boldsymbol{X}$ and the estimated symmetric shape.

Analyzing asymmetry: a resistant method

Available formulations of resistant Procrustes methods in a more general shape analysis context [20,21,22] suggest that a resistant approach to the specific study of shape asymmetry could also be offered. A resistant method might bring insightful information on the pattern of symmetry departures at least as an exploratory tool, and the framework presented in this article takes the challenge.

The estimation of the symmetric shape is a central step in assessing asymmetry when the standard LS Procrustes method is used. The resistant method focuses on the same target, which in turn will enable a more comprehensive measurement of asymmetry.

Matching symmetry

A resistant Procrustes procedure to identify and measure via landmarks departures from symmetry within individuals for two-dimensional structures exhibiting matching symmetry is presented next. For simplicity, geometric shapes are used to illustrate the method: two mirror copies of a 18-landmark letter "R" were chosen. To simulate localized asymmetry, landmarks 2-3 and 11-12-13 were randomly distorted in each of them (Figure 1A).

(i) Compute any of these two location centers, the *componentwise median* (*cmed*) (darkest dots, Figure 1A) or the *spatial median* (*smed*), for both landmark configurations. Both are reasonable choices as multivariate resistant location centers because they generalize the univariate median according to different critera:

• *cmed* [32] is the point that divides the corresponding landmark configuration in halves along the direction of every coordinate axis (i.e., either an horizontal or a vertical line through the cmed leaves 50% of the points on one side and the remaining 50% on the opposite side)

• *smed* [22,34] is the point that minimizes the sum of non-squared Euclidean distances to every landmark in the configuration.

Once the same resistant location center has been computed for both sides, translate each of them to place their common center at the origin (resistant centering) (Figure 1B). (Note that both resistant centerings could be

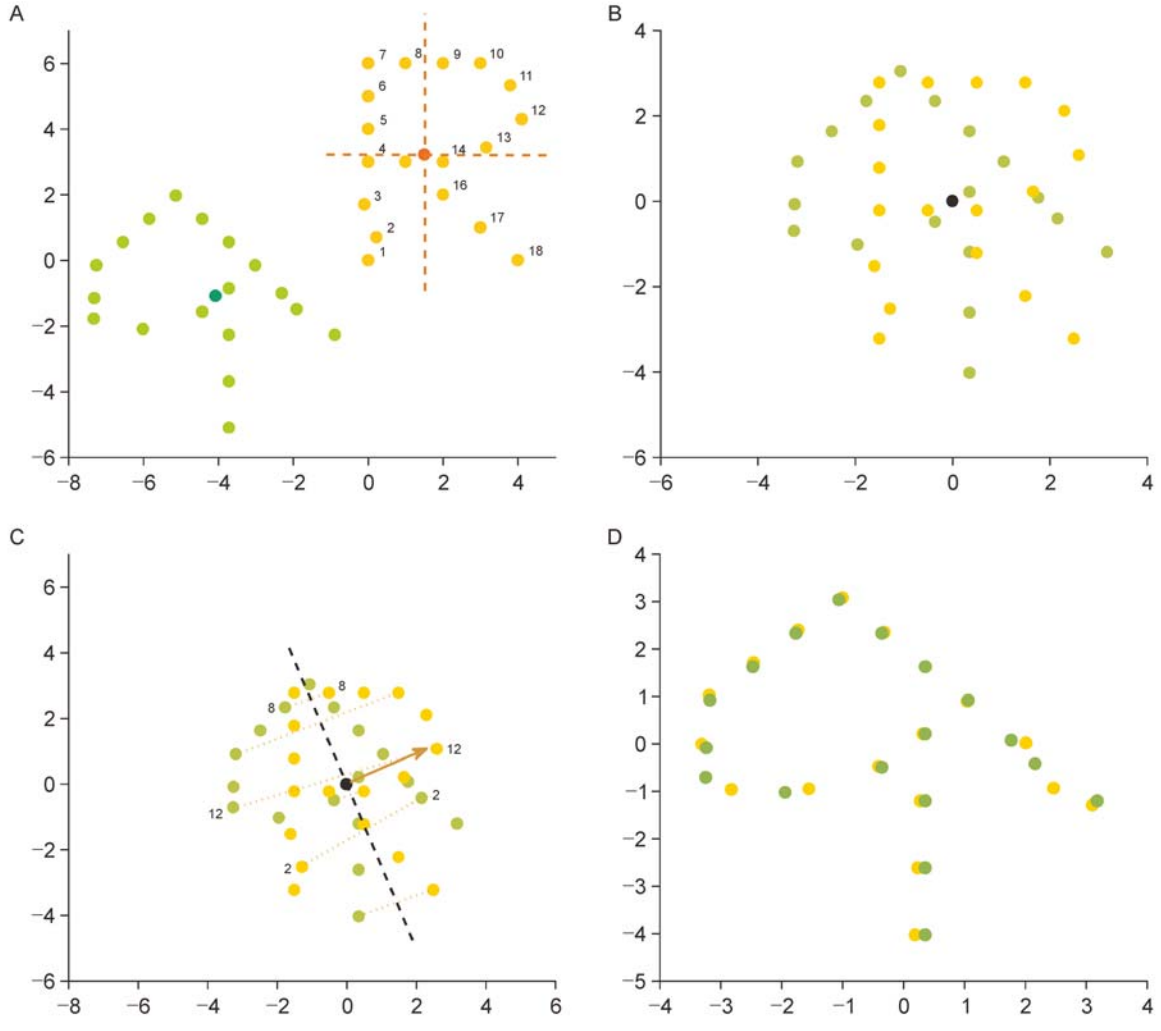

Figure 1. Steps for the resistant analysis of matching symmetry. (A) The same resistant location center (darkest dots) is computed for both mirror copies. (B) Configurations are translated to place their corresponding resistant center (black dot) at the origin of coordinates. (C) Difference vectors (dotted lines) are first normalized, and their sphmed (arrow) is afterwards computed. The estimated resistant median axis (dashed line) is the line perpendicular to sphmed. (D) Any of the copies (the yellow one in this case) is reflected about the estimated median axis. An additional resistant Procrustes superimposition filters out the eventually remaining differences due to scale and/or orientation.

tried in an exploratory analysis, and their results afterwards compared)

(ii) Compute the difference vectors between the landmarks from one side and the corresponding landmarks from the other side (e.g., vectors going from right landmarks to left ones; dotted lines, Figure 1C) and divide each of them by the respective length to produce unit-length difference vectors. These vectors lie on the unitary circumference and can be thought as representing directions in two dimensions, which due to matching symmetry are approximately parallel to each other.

(iii) Compute the *spherical median* (*sphmed*) [35] from all these directions, which is also a unit-length vector that minimizes the sum of arc-distances over the unitary circumference to all of them. From a resistant point of view, the sphmed (arrow, Figure 1C) is the direction that best summarizes the whole set of difference directions.

(iv) Take the line through the origin that is perpendicular to the sphmed direction as the resistant median axis (dashed line, Figure 1C) and reflect about it one side onto the other, thus leaving both sides with the same orientation (Figure 1D)

(v) Perform an resistant Procrustes superimposition [22], which by construction does not include a reflection, to filter out the possibly remaining differences in size and/or orientation between sides (Figure 2, left)

(vi) Compute the resistant symmetric shape as the *row-wise spatial median* [22] (agrees with the average in case of two configurations) from the optimally fitted sides. A resistant measure of asymmetry is afterwards given by the sum of non-squared Euclidean distances across corresponding landmarks between the optimally fitted configurations or, equivalently (up to a factor of 2), by the sum of non-squared Euclidean distances across corresponding landmarks between one of the fitted configurations and the estimated symmetric shape. This measure is a resistant shape distance [22] where each landmark contributes the corresponding term in the sum. Moreover, this contribution simply quantifies the residual or misfit for each landmark that is readily seen when the results are graphically depicted (Figure 2, left). When this contribution is expressed as a percentage (Table 1), the degree of asymmetry accounted for by each landmark is revealed.

Object symmetry

A resistant Procrustes procedure to analyze and measure via landmarks departures from symmetry within individuals for two-dimensional structures exhibiting object symmetry is now presented. Geometric shapes are again used for illustration: a 15-landmark letter "Y" consisting of 5 unpaired and 10 paired landmarks was chosen. To simulate a localized pattern of asymmetry (Figure 3A, random distortion was introduced in unpaired landmarks 1 and 4 and paired ones 7, 8, 12 and 13 (lower distortion was used for the unpaired landmarks to be more realistic).

(i) For the given landmark configuration $\boldsymbol{X}$, compute any of the two resistant location centers previously described: the componentwise median *cmed* (red dot, Figure 3B) or the spatial median *smed*. Translate the configuration to place its resistant location center at the origin (Again, both alternatives could be tried in an exploratory analysis).

(ii) For every pair of unpaired landmarks compute the corresponding difference vector and divide it by its length, obtaining in this way unit-length unpaired difference vectors (arrows, Figure 3C) or unpaired

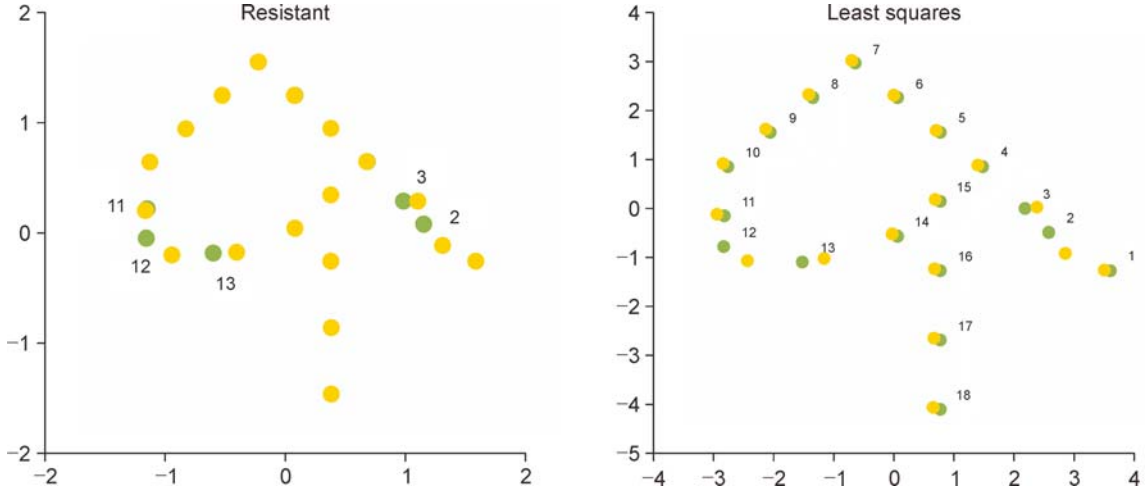

Figure 2. Matching symmetry: fitted configurations by using the resistant (left) and the LS (right) Procrustes method. A resistant measure of asymmetry is given by the sum of non-squared Euclidean distances across landmarks, where each landmark contributes the corresponding proportion of exhibited lack of fit. The resistant symmetric shape (not shown) is the row-wise spatial median from the matched configurations.

Table 1. Matching symmetry geometric example.

Landmark	Contribution % to asymmetry (Res)	Contribution % to asymmetry (LS)
1	0.0668	3.3492
2	28.9533	17.0307
3	14.1879	6.6644
4	0.0325	2.9273
5	0.0387	2.8304
6	0.0482	2.7569
7	0.0663	2.7147
8	0.0602	2.9986
9	0.0611	3.2828
10	0.0656	3.567
11	2.5674	4.2481
12	30.5805	16.6064
13	23.1067	12.5457
14	0.0098	3.458
15	0.0114	3.1926
16	0.0189	3.5635
17	0.0477	3.9408
18	0.0770	4.3228
	100.0000	100.0000

Contribution % by landmark to asymmetry for the resistant (Res) and LS results displayed in Figure 2. Total asymmetry was computed in both cases as the sum of non-squared Euclidean distances across landmarks (i.e., the visible asymmetry) between the matched configurations.

directions. Since by object symmetry all unpaired landmarks approximately lie on the (unknown) median axis, these unpaired directions are approximations of the median axis and thus approximately perpendicular to all difference vectors between paired landmarks

(iii) For every pair of paired landmarks now compute the corresponding paired difference vector, not dividing it by its length. As mentioned, due to object symmetry these paired differences vectors (dotted lines, Figure 3D) are approximately perpendicular to the (unknown) median axis or, equivalently, their projections onto the (unknown) median axis are approximately zero.

(iv) Pick each unpaired direction at a time, and project all paired differences onto it computing the sum (or the median) of the resulting projection lengths (red lines, Figure 3E). A rank of the unpaired directions can be given based on these sums (or medians). Obtain also the sphmed direction from the unpaired directions and project all paired differences onto it, compute the corresponding sum (or median) of the projection lengths and rank it among those from all the unpaired difference vectors.

(v) The direction of the unpaired difference or the sphmed achieving the least sum (or median) of projections is chosen as the resistant median axis (dashed line, Figure 3E): by construction, it enjoys two desirable and intuitive geometrical properties: 1) it is based on unpaired landmarks, which by definition lie approximately on the median axis; and 2) by minimizing the sum (median) of the projection lengths from all the paired differences, it is approximately perpendicular to all such paired differences.

(vi) Use the resistant median axis estimated from the previous step, which goes through the origin of Coordinates, to produce a reflected copy $\boldsymbol{Z}$ (open dots, Figure 3F) of the original configuration $\boldsymbol{X}$. Relabel each paired landmark in $\boldsymbol{Z}$ to make the corresponding rows from $\boldsymbol{X}$ and $\boldsymbol{Z}$ describe landmarks on the same side from the median axis.

(vii) Compute the *resistant symmetric shape* (green dots, Figure 4 left) as the *row-wise spatial median* between the original and the reflected configurations. Landmarks (rows) from this spatial median configuration [22]; agrees with the average in case of two configurations) are, by contruction, equidistant from the corresponding original and reflected landmarks thus resulting in a perfectly symmetric configuration. A resistant measure of asymmetry is afterwards given by the resulting sum of non-squared Euclidean distances across corresponding landmarks between the original and the reflected configuration or, equivalently (up to a factor of 2), by the sum of non-squared Euclidean distances across corresponding landmarks between the original configuration (orange dots, Figure 4 left) and the estimated symmetric shape (green dots, Figure 4 left). Just as in

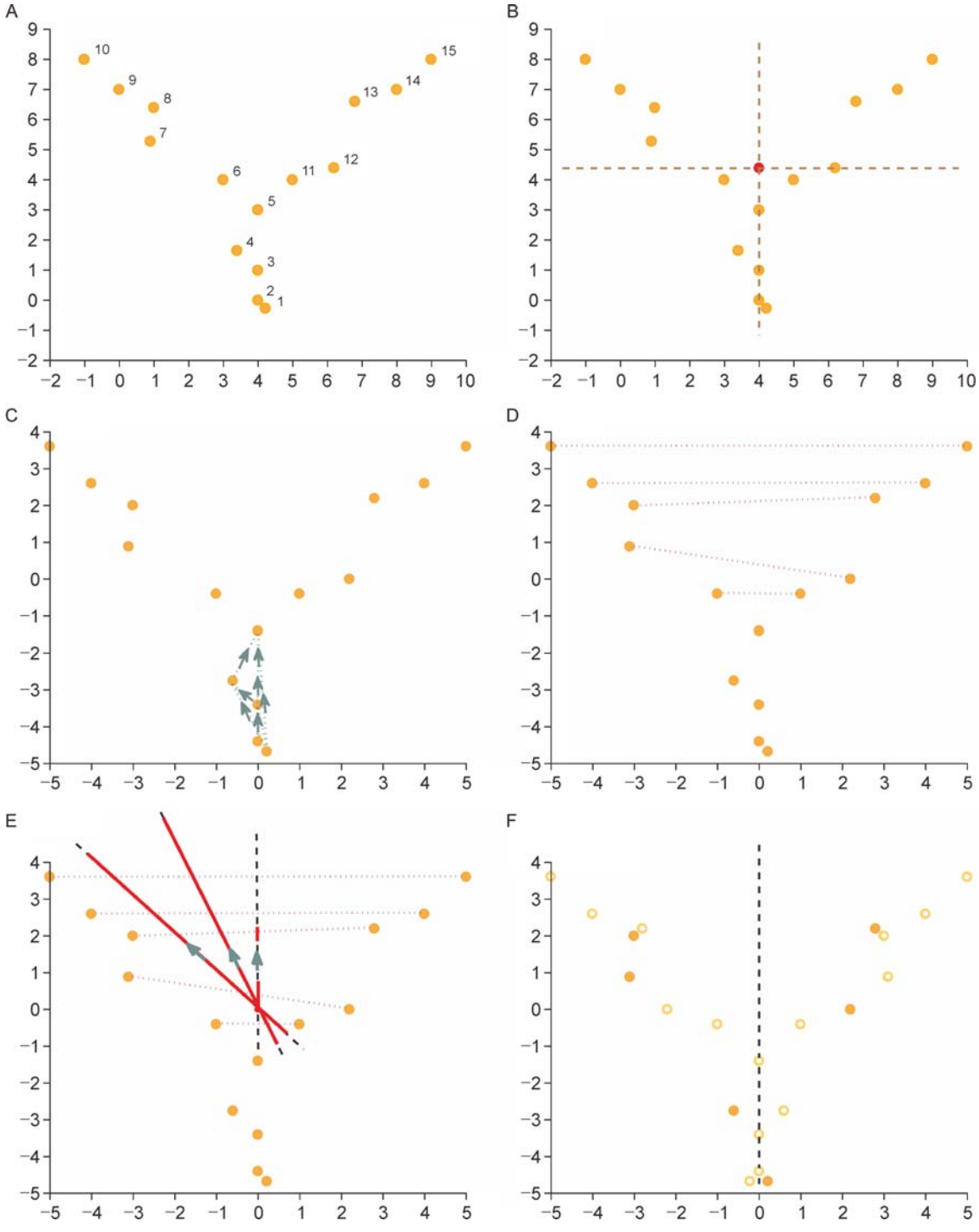

Figure 3. Steps for the resistant analysis of object symmetry. (A) The structure consists of unpaired landmarks 1 to 5, and paired landmarks 6–11, 7–12, 8–13, 9–14, 10–15. (B) A resistant location center (red dot) is computed and the configuration is afterwards translated to place this resistant center at the origin of coordinates. (C) For every pair of unpaired landmarks, the corresponding unit-length direction vectors (arrows) are computed. (D) For every pair of paired landmarks, the corresponding difference vectors (dotted lines) are computed. (E) All paired differences are projected onto every unpaired direction and onto their sphmed direction also (arrows), and the corresponding sum of projection lengths (red lines) is computed. The unpaired or sphmed direction achieving the least sum of projections lengths is the estimated median axis (dashed line). (F) The original configuration (filled dots) is reflected (open dots) about the estimated median axis. The resistant symmetric shape (not shown) is the row-wise spatial median from the original and the reflected configurations.

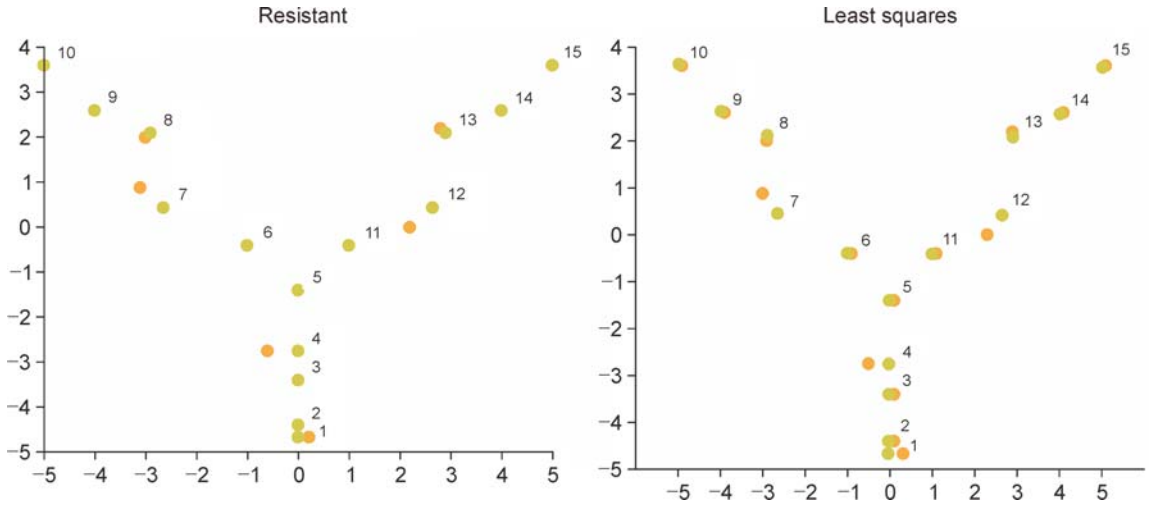

Figure 4. Object symmetry: original configuration (orange dots) and the estimated symmetric shape (green dots) when the resistant (left) and the LS (right) Procrustes methods are used. Resistant asymmetry is measured through the sum of non-squared Euclidean distances across landmarks between them; each landmark contributes the proportion of displayed lack of fit in the overall sum.

the matching symmetry case, the contribution percentage to asymmetry accounted for by each landmark can be obtained (Table 2).

Comparison of methods in biological examples

Simulated biological examples based on real data are now considered. For each type of bilateral symmetry, the standard LS and the introduced resistant Procrustes method were applied in order to compare their results.

Matching symmetry

The wings of a *Drosophila melanogaster* (Figure 5) were

Table 2. Object symmetry geometric example.

Landmark	Contribution % to asymmetry (Res)	Contribution % to asymmetry (LS)
1	9.3158	11.4231
2	0.0000	4.2057
3	0.0000	3.9795
4	25.4068	15.6850
5	0.0000	3.5271
6	0.0000	3.3087
7	26.6502	17.9146
8	5.9884	3.9430
9	0.0000	2.7740
10	0.0000	2.6496
11	0.0000	3.3087
12	26.6502	17.9146
13	5.9884	3.9430
14	0.0000	2.7740
15	0.0000	2.6496
	100.0000	100.0000

Contribution % by landmark to asymmetry for the resistant (Res) and LS results displayed in Figure 4. Total asymmetry was computed in both cases as the sum of non-squared Euclidean distances across landmarks (i.e., the visible asymmetry) between the original configuration and the estimated symmetric shape.

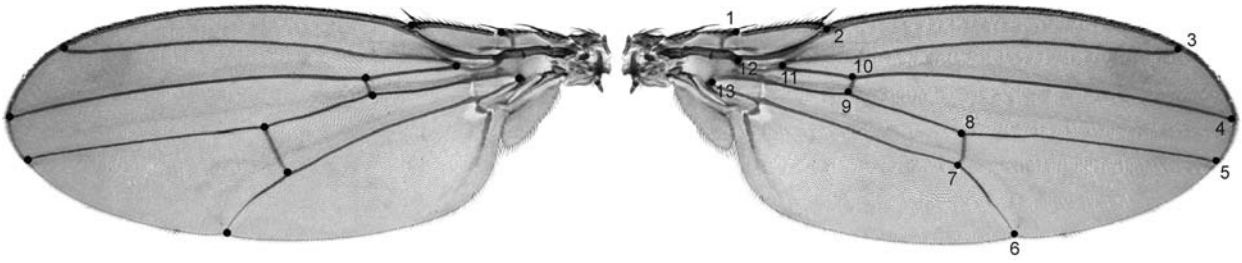

Figure 5. Simulated biological example of matching symmetry: digitized landmarks from *Drosophila melanogaster* wings. Asymmetry between sides was artificially introduced in landmarks 7, 8, 9, 10 and 13.

used for matching symmetry simulation. Thirteen landmarks were digitized; eight of them were perfectly symmetric while symmetry distortion was randomly introduced in landmarks 7, 8, 9, 10 and 13. The estimated symmetric shape (orange dots) versus one of the fitted configurations (black dots) by using the LS and resistant methods are displayed in Figure 6.

As shown, all landmarks exhibit some departure from the estimated symmetric shape when the standard LS method is used (Figure 6, top). Based on this overall lack of fit it is inferred that every landmark is contributing to asymmetry to varying degrees.

The resistant Procrustes method (Figure 6, bottom) estimates instead a symmetric shape that almost perfectly covers those landmarks with no symmetry distortion; a clear residual is thus exhibited for the few points deviating from symmetry.

This visual impression can be accordingly quantified by computing the contribution percentage accounted for by each landmark to the measured and visible asymmetry (Table 3). Note that those landmarks with a prominent role in explaining asymmetry can be readily drawn from the resistant (Res) contributions list by their highest percentages. This is not easily seen by checking the LS contributions; moreover, the LS method wrongly identifies landmark 7 as the location most deviating from symmetry (which in fact occurs at landmarks 9 and 10) and misses landmark 13 moderate asymmetry contribu-

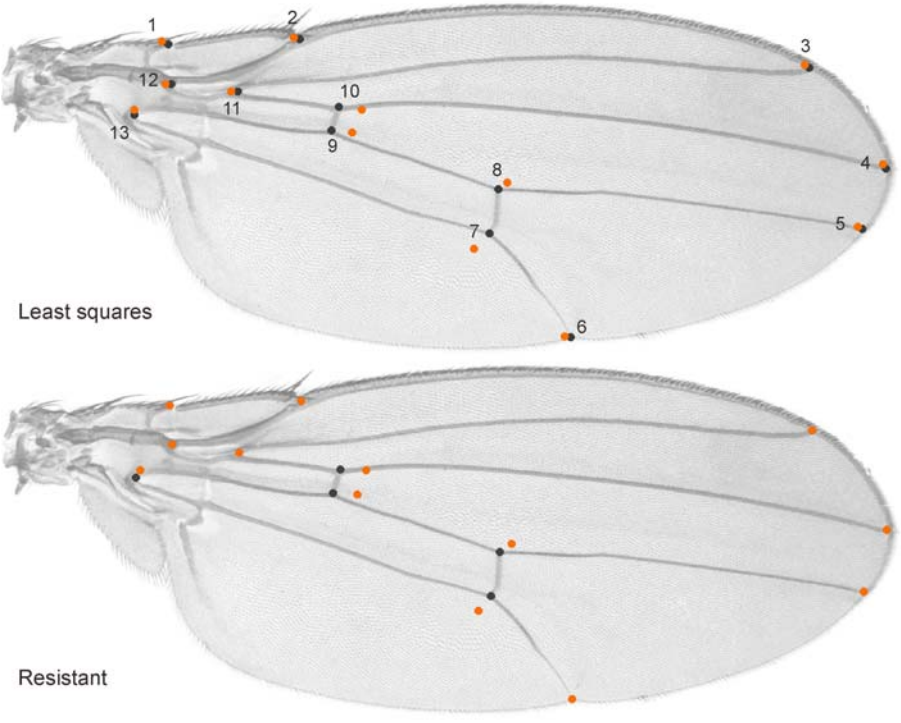

Figure 6. Resistant vs LS results for the *Drosophila melanogaster* wings. One of the configurations (black dots) and the estimated symmetric shape (orange dots) are shown.

Table 3. Matching symmetry biological example (*Drosophila* wings).

Landmark	Contribution % to asymmetry (Res)	Contribution % to asymmetry (LS)
1	1.6566	6.2517
2	1.8427	6.6286
3	0.7217	5.4708
4	1.1847	5.7650
5	0.7929	5.9256
6	0.8393	5.9218
7	20.163	17.358
8	14.014	6.0611
9	24.716	11.6390
10	26.223	12.6910
11	0.1862	5.5184
12	0.8967	5.3457
13	6.7633	5.423
	100.0000	100.0000

Contribution % by landmark to asymmetry for the resistant (Res) and LS results displayed in Figure 6 . Total asymmetry was computed in both cases as the sum of non-squared Euclidean distances across landmarks (i.e., the visible asymmetry) between the matched configurations

tion, which is probably lost in the overall misfit.

Object symmetry

For object symmetry simulation, human face data were used. Twenty landmarks, six unpaired (landmarks 1 to 6) and seven pairs (landmarks 7 to 20), were digitized in facial traits such as the corners of eyes, nose and mouth, and the tip of nose and chin (Figure 7) . Among them, thirteen landmarks were perfectly symmetric while artificial distortion (lower for paired ones) was randomly intoduced in unpaired landmarks 4 and 5 and paired ones 7, 16, 17, 18 and 19.

The original configuration (black dots) and the estimated symmetric shape (orange dots) are shown in Figure 8. As is usually the case whenever localized shape variation is present, an overall misfit about the symmetric shape is exhibited following a LS Procrustes superimposition. Again, this result suggests that every landmark is contributing to asymmetry to some extent (Figure 8, right).

The resistant method (Figure 8, left), in turn, estimates a median axis and a corresponding symmetric shape that passes through most unpaired landmarks: the undistorted ones. A readily and more accurate identification of the least symmetrical locations is therefore obtained because a clear lack of fit is shown basically for the few landmarks deviating from symmetry.

When the visual impression is quantified by computing the asymmetry contribution percentage (Table 4), following a LS approach some landmarks turn out to contribute much more (e.g., unpaired landmark 6, paired landmarks 13-20) or much less (e.g., paired landmarks 7-14) than

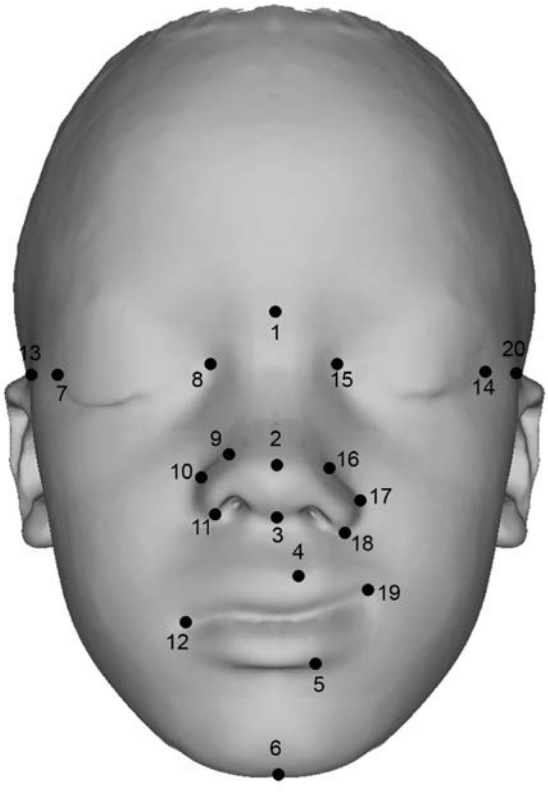

Figure 7. Simulated biological example of object symmetry: digitized landmarks from a human face. Landmarks 1 to 6 are unpaired, and paired landmarks are 7-14, 8-15, 9-16, 10-17, 11-18, 12-19 and 13-20. Asymmetry was artificially introduced in unpaired landmarks 4 and 5 and in paired ones 7, 16, 17, 18 and 19.

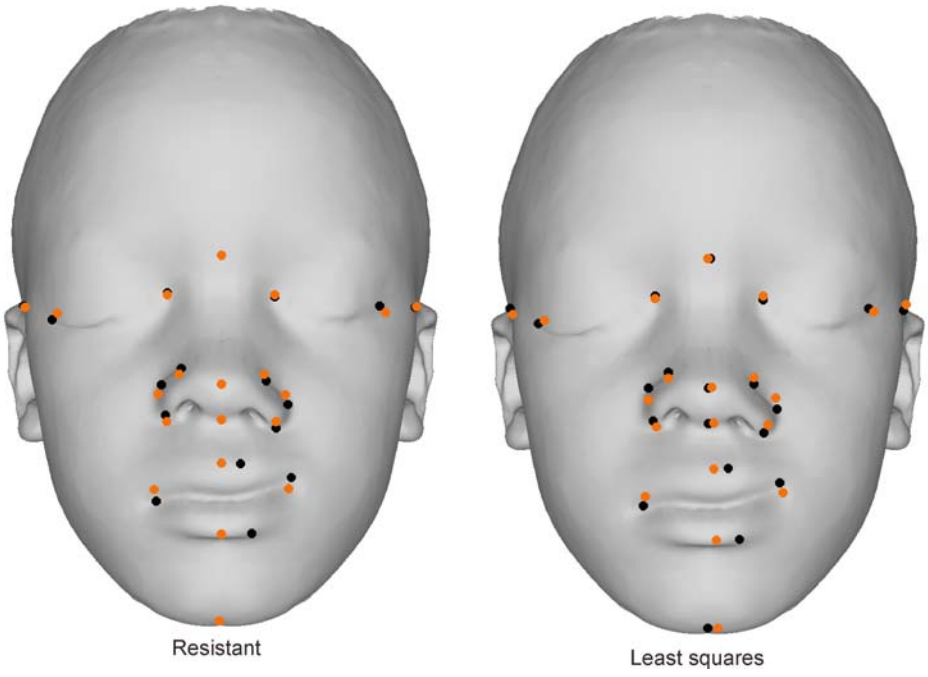

Figure 8. Resistant vs LS results for the human face. The original configuration (black dots) and the estimated symmetric shape (orange dots) are shown.

Table 4. Object symmetry biological example (human face).

Landmark	Contribution % to asymmetry (Res)	Contribution % to asymmetry (LS)
1	0.0000	0.7883
2	0.0000	1.3007
3	0.0000	1.8856
4	13.2750	9.4706
5	20.6000	14.9791
6	0.9155	6.0078
7	6.3636	4.1969
8	0.5118	1.2582
9	4.3428	4.4145
10	7.4554	7.4663
11	4.1453	5.1682
12	8.6189	6.8189
13	1.1671	3.4610
14	6.3636	4.1969
15	0.5118	1.2582
16	4.3428	4.4145
17	7.4554	7.4663
18	4.1453	5.1682
19	8.6189	6.8189
20	1.1671	3.4610
	100.0000	100.0000

Contribution % by landmark to asymmetry for the resistant (Res) and LS results displayed in Figure 8. Total asymmetry was computed in both cases as the sum of non-squared Euclidean distances across landmarks (i.e., the visible asymmetry) between the original configuration and the estimated symmetric shape.

expected. This is caused by the impact of the neighboring highly asymmetric landmarks allowed by the LS method when averaging. The resistant (Res) contributions, conversely, effectively reflect the degree of asymmetry seen for every landmark. Note that paired landmarks always share their contribution (either Res or LS) because the estimated symmetric shape equally distributes their asymmetry.

DISCUSSION

It is acknowledged within geometric morphometrics that the quantitative description of shape may be approached according to different paradigms [9,16,20–22,31–33], each of them having the corresponding biological implications. The specific field of shape asymmetry analysis is not an exception, and this work claims that the use of a resistant approach may bring insightful information to address a wide range of biological or medical problems.

This article introduces a resistant method for studying individual shape asymmetry in two dimensions, whose formulation is more grounded on the geometry of data. Simulated examples suggested that resistant method results agree with visual impressions: the most asymmetric (symmetric) landmarks can be readily identified by their large (small) residuals, which in turn helps symmetry departures to be more easily understood. The worked examples also showed that by limiting the effect of highly asymmetric points, the symmetric shape is more effectively estimated and asymmetry is therefore more accurately measured when the resistant method is used. In addition, a revealing measure such as the contribution percentage to measured asymmetry accounted for by each landmark can be computed; this useful tool provides an objective basis for a comprehensive characterization of the measured (and exhibited) asymmetry.

Overall, the resistant method is a useful exploratory tool which may be the preferable method whenever a non homogeneous deformation of bilateral symmetric structures is possible (e.g., skulls with craniosynostosis). By offering a more detailed analysis and a rather exhaustive explanation of the asymmetry pattern, the resistant approach may indeed contribute to improve the quality of biological or developmental inferences. Worth noting that the specific formulation of the resistant method presented here neither requires a standard LS Procrustes superimposition to be performed first nor is benefited from such a preliminary LS fit; this is a slightly different situation from more general shape analyses [20–22].

The LS Procrustes method is commonly used and has proven useful in the study of shape asymmetry; it is not implied here that a resistant approach should replace it at all. Instead, researchers are invited to keep asking questions about their data and try to avoid blindly applying techniques that often produce misleading results. Different symmetric shape estimates and hence different inferences can be drawn by using different methods. As the pioneer in robust statistics John Tukey once said, it is perfectly proper to use both LS and resistant methods routinely and only worry when they differ enough to matter. But when they do differ, researchers must think hard. Modern morphologists are thus encouraged to increase their statistical training, not only to gain insight into the methods they use but also to apply and eventually conceive alternative ones.

A resistant analysis of symmetry departures for individual biological structures could be particularly useful in many actual situations: e.g., to help diagnosis when asymmetry is linked to some type of illness or pathology (brain asymmetrical pathology in neurodegenerative diseases, mandibular asymmetry causing dentofacial asymmetry). When asymmetry analyses are based on populations rather than on single individuals, specific types of asymmetry such as directional asymmetry, fluctuating asymmetry and antisymmetry [7,8,11,12,15] are distinguished and their implications studied accordingly. A general strategy to perform a resistant study of asymmetry in such context, either for two or three dimensional data, could complete the ideas introduced here and it is hoped that a future work will entail this target.

METHODS

All methods used were implemented in Scilab (free and open source software for numerical computation) 5.5.2 for 64-bit Windows, available from http://www.scilab.org

COMPLIANCE WITH ETHICS GUIDELINES

Sebastián Torcida, Paula Gonzalez and Federico Lotto declare that they have no conflict of interest.

This article does not contain any studies with human or animal subjects performed by any of the authors.

REFERENCES

1. Debat, V., Milton, C. C., Rutherford, S., Klingenberg, C. P. and Hoffmann, A. A. (2006) Hsp90 and the quantitative variation of wing shape in *Drosophila melanogaster*. Evolution, 60, 2529–2538
2. Gonzalez, P. N., Lotto, F. P. and Hallgrímsson, B. (2014) Canalization and developmental instability of the fetal skull in a mouse model of maternal nutritional stress. Am. J. Phys. Anthropol., 154, 544–553
3. Willmore, K. E., Leamy, L. and Hallgrímsson, B. (2006) Effects of developmental and functional interactions on mouse cranial variability through late ontogeny. Evol. Dev., 8, 550–567
4. Palmer, A. R. and Strobeck, C. (1986) Fluctuating asymmetry: measurement, analysis, patterns. Annu. Rev. Ecol. Syst., 17, 391–421
5. Adams, D. C., Rohlf, F. J. and Slice, D. E. (2004) Geometric

morphometrics: ten years of progress following the 'revolution'. Ital. J. Zool., 71, 5–16

6. Adams, D. C., Rohlf, F. J. and Slice, D. E. (2013) A field comes of age: geometric morphometrics in the twenty first century. Hystrix, 24, 7–14
7. Auffray, J. C., Alibert, P., Renaud, S., Orth, A. and Bonhomme, F. (1996). Fluctuating asymmetry in mus musculus sub-specific hybridization: traditional and Procrustes comparative approach. In Advances in Morphometrics. Marcus, L. F. *et al*. eds., 275–283. New York: Plenum Press
8. Auffray, J. C., Debat, V. and Alibert, P. (1999) Shape asymmetry and developmental stability. In On Growth and Form: Spatio-temporal Pattern Formation in Biology. Chaplain, M. A. J. *et al*. eds., 309–324. Chichester: Wiley
9. Bookstein, F. L. (1996a) Biometrics, biomathematics and the morphometric synthesis. Bull. Math. Biol., 58, 313–365
10. Bookstein, F. L. (1996b). Combining the tools of geometric morphometrics. In Advances in Morphometrics. L. F. Marcus, L. F. *et al*. eds., 131–151, New York: Plenum Press
11. Klingenberg, C. P., Barluenga, M. and Meyer, A. (2002) Shape analysis of symmetric structures: quantifying variation among individuals and asymmetry. Evolution, 56, 1909–1920
12. Klingenberg, C. P. (2015) Analyzing fluctuating asymmetry with geometric morphometrics: concepts, methods, and applications. Symmetry, 7, 843–934
13. Mardia, K. V., Bookstein, F. L. and Moreton, I. J. (2000) Statistical assessment of bilateral symmetry of shapes. Biometrika, 87, 285–300.
14. Mitteroecker, P. and Gunz, P. (2009) Advances in geometric morphometrics. Evol. Biol., 36, 235–247
15. Smith, D. R., Crespi, B. J. and Bookstein, F. L. (1997) Fluctuating asymmetry in the honey bee, *Apis mellifera*: effects of ploidy and hybridization. J. Evol. Biol., 10, 551–574
16. Catalano, S. A. and Goloboff, P. A. (2012) Simultaneously mapping and superimposing landmark configurations with parsimony as optimality criterion. Syst. Biol., 61, 392–400
17. Richtsmeier, J. T., DeLeon, V. B. and Lele, S. R. (2002) The promise of geometric morphometrics. Am. J. Phys. Anthropol., 119, 63–91
18. Theobald, D. L. and Wuttke, D. S. (2006) Empirical Bayes hierarchical models for regularizing maximum likelihood estimation in the matrix Gaussian Procrustes problem. Proc. Natl. Acad. Sci. USA, 103, 18521–18527
19. Van der Linde, K. and Houle, D. (2009) Inferring the nature of allometry from geometric data. Evol. Biol., 36, 311–322
20. Siegel, A. F. and Benson, R. H. (1982) A robust comparison of biological shapes. Biometrics, 38, 341–350
21. Slice, D. E. (1996). Three-dimensional generalized resistant fitting and the comparison of least-squares and resistant fit residuals. In Advances in Morphometrics, Marcus, L. F. *et al*. eds., 179–199, New York: Plenum Press
22. Torcida, S., Perez, I. and Gonzalez, P. N. (2014) An integrated approach for landmark-based resistant shape analysis in 3D. Evol. Biol., 41, 351–366
23. Hampel, F. R., Ronchetti, E. M., Rouseeuw, P. J. and Stahel, W. A. (1986) Robust Statistics: The Approach Based on Influence Functions. New York: Wiley
24. Huber, P. (1981) Robust Statistics. New York: Wiley
25. Siegel, A. F. (1982) Robust regression using repeated medians. Biometrika, 69, 242–244
26. Klingenberg, C. P. and McIntyre, G. S. (1998) Geometric morphometrics of developmental instability: analyzing patterns of fluctuating asymmetry with Procrustes methods. Evolution, 52, 1363–1375
27. Cheverud, J. (1995) Morphological integration in the saddleback tamarin (*Saguinus fuscicollis*) cranium. Am. Nat., 145, 63–89
28. Hallgrímsson, B. and Lieberman, D. E. (2008) Mouse models and the evolutionary developmental biology of the skull. Integr. Comp. Biol., 48, 373–384
29. Zelditch, M. L., Swiderski, D. L., Sheets, H. D. and Fink, W. L. (2004) Geometric Morphometric for Biologists. London: Academic Press
30. Slice, D. E. (2001) Landmark coordinates aligned by procrustes analysis do not lie in Kendall's shape space. Syst. Biol., 50, 141–149.
31. Gower, J. C. (1975) Generalized procrustes analysis. Psychometrika, 40, 33–51
32. Rohlf, F. J. and Slice, D. E. (1990) Extensions of the Procrustes method for the optimal superimposition of landmarks. Syst. Zool., 39, 40–59
33. Bookstein, F. L. (1991) Morphometric Tools for Landmark Data: Geometry and Biology. New York: Cambridge University Press
34. Weiszfeld, E. (1937) On the point for which the sum of the distances to n given points is minimum. Tohoku Math. J., 43, 355–386
35. Xue, G. L. (1994) A globally convergent algorithm for facility location on a sphere. Comput. Math. Appl., 27, 37–50

